Life-Cycle Analysis Results for Geothermal Systems in Comparison to Other Power Systems: Part II

Energy Systems Division

Life-Cycle Analysis Results for Geothermal Systems in Comparison to Other Power Systems: Part II

by
J.L. Sullivan, C.E. Clark, L. Yuan, J. Han, and M. Wang
Energy Systems Division, Argonne National Laboratory

November 2011

CONTENTS

FIGURES

FIGURES (Cont.)

TABLES

LIFE-CYCLE ANALYSIS RESULTS FOR GEOTHERMAL SYSTEMS IN COMPARISON TO OTHER POWER SYSTEMS: PART II

J.L. Sullivan, C.E. Clark, L. Yuan, J. Han, and M. Wang

ABSTRACT

A study has been conducted on the material demand and life-cycle energy and emissions performance of power-generating technologies in addition to those reported in Part I of this series. The additional technologies included concentrated solar power, integrated gasification combined cycle, and a fossil/renewable (termed hybrid) geothermal technology, more specifically, co-produced gas and electric power plants from geo-pressured gas and electric (GPGE) sites. For the latter, two cases were considered: gas and electricity export and electricity-only export. Also modeled were cement, steel and diesel fuel requirements for drilling geothermal wells as a function of well depth. The impact of the construction activities in the building of plants was also estimated. The results of this study are consistent with previously reported trends found in Part I of this series. Among all the technologies considered, fossil combustion-based power plants have the lowest material demand for their construction and composition. On the other hand, conventional fossil-based power technologies have the highest greenhouse gas (GHG) emissions, followed by the hybrid and then two of the renewable power systems, namely hydrothermal flash power and biomass-based combustion power. GHG emissions from U.S. geothermal flash plants were also discussed, estimates provided, and data needs identified. Of the GPGE scenarios modeled, the all-electric scenario had the highest GHG emissions. Similar trends were found for other combustion emissions.

1 INTRODUCTION

Geothermal power production represents a set of technologies being explored as alternatives to producing electricity by more conventional means. The intent of this study is to identify environmentally acceptable approaches to power provision with a much-reduced carbon footprint and fossil-fuel dependence. This report is an extension of a previously published life-cycle analysis (LCA) (Sullivan et al., 2010) on geothermal electricity production. The original report, henceforth denoted as Part I, reviewed the LCA literature on power plants with a special emphasis on comparing the environmental performance of geothermal power to that of other power production systems, such as conventional fossil, nuclear, and renewable-based methods. After normalizing identified life-cycle burdens (energy and carbon dioxide) on the basis of a common functional unit, in this case lifetime kilowatt-hours (kWh) generated, the relative environmental performances of the different generating technologies were compared.

Part I also focused on the determination of the magnitude of plant cycle-stage burdens on LCA results relative to those for the total life cycle, taken to be the sum of burdens for the plant cycle, fuel production, and fuel use stages. Sometimes plant cycle energy, E_{pc}, is termed embodied energy; we use both terms interchangeably. Plant cycle burdens have both direct and indirect components. The former include those associated with plant construction activities such as excavation, building erection, operation of cranes, transport of building materials to the site, and others, while the latter accounts for the production of materials that comprise plant structures and components (turbines, generators, buildings, boilers, dams, and others). Part I covered only indirect E_{pc} burdens.

The purpose of this report is to expand the results of Part I to include LCA information on three additional power-generating technologies: i.e., geo-pressured gas and electric (GPGE) wells that produce both natural gas and electricity, integrated gasification combined cycle (IGCC) plants fired by coal and biomass, and concentrated solar power (CSP) plants. Given that plant cycle components of the total life-cycle energy and greenhouse gas (GHG) emissions are comparatively large for geothermal power, we present new results for this stage of geothermal systems. More specifically, life-cycle results are presented for 1) well material and fuel requirements as a function of well depth and technology, 2) the impact of well-field exploration on well-field life-cycle burdens, and 3) the contribution of on-site plant construction activities to E_{pc}. As emissions are also an important environmental metric for power production, results are presented on the range of GHG emissions from U.S. geothermal power facilities. Finally, other combustion emissions are compared and contrasted among the various power production technologies. For a detailed discussion of the considerable water requirements for drilling geothermal wells, see the companion report (Clark et al., 2011b).

2   METHOD

As was pointed out before (Sullivan et al., 2010), a key component of any life-cycle assessment is a statement of system boundaries. It is difficult at best to compare study results without clearly defined boundaries. A significant component of observed variances between studies often arises from differences in system definition.

The system boundary for our study is depicted in Figure 1. In our previous study, the system product was a lifetime of kWh delivered to the grid. However, for this study, the system product is expanded to include systems delivering more than one energy output, such as geo-pressured gas and electricity. As the figure shows, the life-cycle stages defined as "covered" in our study are fuel production, fuel use (plant operation), and plant construction. A life-cycle stage not shown in the figure is plant decommissioning and recycling. Because this stage generally makes a small contribution to plant cycle results, it was not included in our assessments. See Part I for a more complete discussion of system boundaries
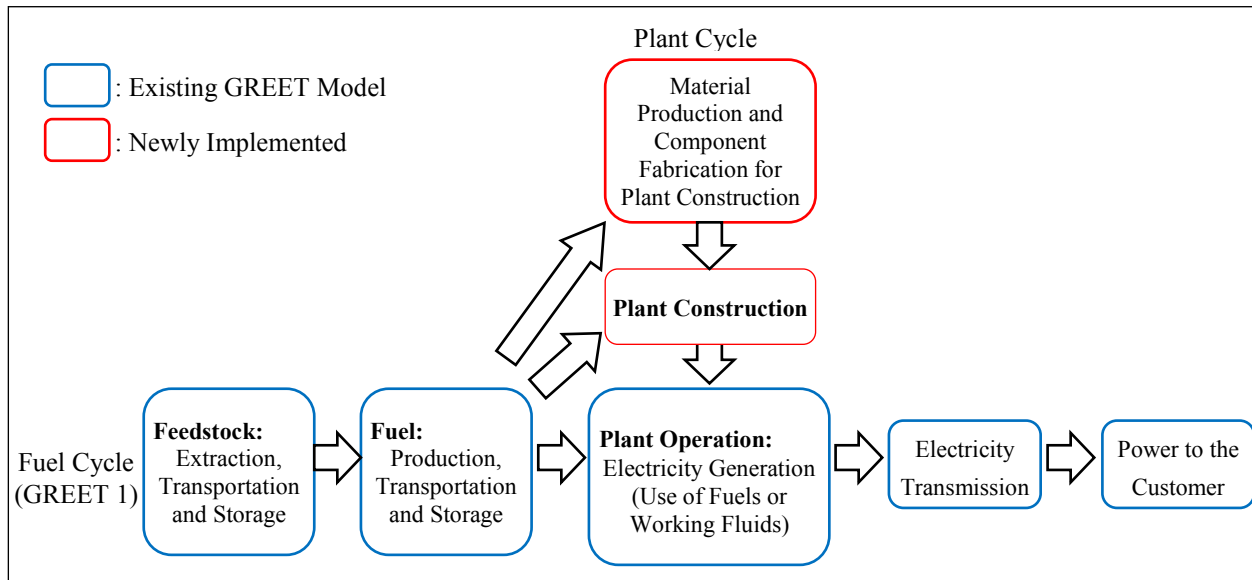
Figure 1   Flowchart of Life-Cycle Analysis

The results presented herein are based on process life-cycle assessment. Previously, we compared three forms of geothermal power production to electricity from coal, natural gas, nuclear, and biomass power plants. Also included in the analysis was electricity from hydroelectric, wind, and photovoltaic (PV) power production facilities. The three geothermal technologies covered were enhanced geothermal (EGS), hydrothermal flash (HT-Flash), and hydrothermal binary (HT-Binary) power plants. This study extends the range of covered power-generating technologies to include IGCC, CSP, and GPGE. As one of the objectives of our LCAs is to determine E_{pc} and emissions burdens (CO_2 and others), materials required in significant amounts for building the various power plants and auxiliary systems were quantified and

presented on a mass-to-power-plant-capacity ratio (MPR) basis for each technology. From the MPRs, the energy consumed and emissions incurred in providing those materials were computed and represented on a plant lifetime power output basis.

Because the MPRs are normalized by plant power capacity, they are hardware functional units, which represent the material requirements to build a megawatt (MW) of power plant. However, combining these MPRs with plant capacity, lifetime, capacity factor, and the fuel use and emissions incurred during the production of plant constituent materials yields two important service functional units for the plant cycle stage. They are the energy ratio ($\mathcal{E}_{pc} = E_{pc}/E_{out}$) and the CO_2-equivalent specific GHG emissions metric ($GHG_{pc} = \Sigma GHG_i/E_{out}$), where E_{out} is the total energy output from the system over its lifetime. The latter metric is a sum over a number of GHGs in terms of their CO_2-equivalent emissions (GHG_j); in addition to CO_2, the ones of most significance here are methane (CH_4) and nitrous oxide (N_2O). Service functional units represent both system hardware and how it is used. Later in this report, we estimate and compare $\mathcal{E}_{pc}$ and GHG_{pc} values for the various technologies. After that, we compare overall energy consumption and GHG emissions among the technologies.

When a production facility makes more than one product, allocation issues arise in LCAs. In the case of GPGE systems, which produce both gas and electricity from either a new or a reworked geothermal field, assumptions need to be made regarding the attribution of employed materials to particular facilities and energies. Our approach is an incremental one. We assumed that the only new materials to be considered are those required to build the binary power plant itself and any new materials (steel and cement) required to either refurbish an existing well or drill all-new wells on a greenfield site. Surface piping connecting plant and wells was also included. For brevity, we denote these material uses by where they are employed, i.e., as plant, well, or well-to-plant. In the case of a refurbished site, the steel and cement required to build the original wells were allocated to the gas produced prior to the rework; in short, those materials were not included in our accounting. Because there is a considerable difference between the materials required to rework an existing site and to develop a greenfield site, the relative amounts of materials between the topside electric power plant and wells can vary. For simplicity, we assumed that the separation of natural gas from the geofluid is managed by the binary plant's non-condensable gas equipment. Other than this, most topside materials were associated with the electricity generating plant building and equipment (generators, turbines, others); any new steel and cement for wells and well-to-plant pipelines supported both produced electricity and natural gas. For both greenfield and refurbished sites, it was assumed that gas pipelines already exist. Owing to potentially significant differences in material requirements, two scenarios were selected as the focus of our GPGE assessment of dual-output plants (gas and electricity), i.e., refurbished plants (GPGE-rfrb) and greenfield plants (GPGE-gf).

In Part I, MPRs were straightforwardly computed on the basis of facility material requirements divided by the plant's only output, electric power (MW). However, as GPGE systems are more complicated, yielding in this case two energy outputs, a comparable basis is needed for meaningful comparisons among all the energy-producing systems studied. We recognize that not all MW are equal. Gas and electricity are two different forms of energy and are often used in different ways for different purposes. Nevertheless, a common unit is required. Considering that GPGE facilities are likely to be dual-output plants, producing both geofluid-

based electric power to the grid and gas to an already existing pipeline, our approach to computing these MPRs is to sum the output electric power of the geothermal plant (MW_{el}) with the hourly rate of natural gas production in units of megawatts-thermal (MW_{th}) to arrive at a total energy rate, megawatts-mixed (MW_{mx}) for the facility. This is the approach used throughout the report for dual-output plants. Another potential basis of comparison would be revenue streams for plant energy outputs, although generally speaking, economic bases tend not to be used in life-cycle assessment, primarily because of time variations in market prices.

Another feasible GPGE operating scenario would be to use the natural gas on site to generate additional electricity. The resulting MW_{el} output, solely electricity, would be larger than the MW_{el} of dual-output plants but smaller than their MW_{mx}, owing to the heat-to-electricity conversion efficiency from natural-gas combustion. Because this mode of operation requires additional investment in power-generating equipment as well as a source of water for cooling, we view its widespread adoption as unlikely. Nevertheless, in a later section we make MPR, ε_{pc} and GHG_{pc} estimations for the all-electric output case (GPGE-el) and compare them to those from the dual-output plants.

In addition to CH_4 and N_2O, we have conducted a preliminary assessment of the other combustion emissions from electric power plants. These other emissions include volatile organic compounds (VOCs) and four criteria pollutants, namely, nitrogen oxides (NO_x), sulfur oxides (SO_x), carbon monoxide (CO), and particulates (PM). These results were generated using GREET 1.8, MPRs, and other data for the power-generating technologies.

3 LCAs FOR THE ADDITIONAL POWER SYSTEMS

For IGCC plants, two separate fuels were considered, namely, coal and biomass, and for CSP plants, both trough and tower technologies were studied. The wells of the GPGE plants discussed here are artesian and provide both natural gas and hot water at comparatively high pressures. Co-produced hot water from combined oil and gas wells were not considered, given the low geofluid output generally encountered for those systems (Tester et al., 2006).

Depending on the fuel, IGCC can either be a renewable (biomass) or a fossil-based (coal) technology. CSP plants are, by definition, renewable technologies to the extent that solar energy is driving their outputs. In some cases, however, CPS plants operate on natural gas after sundown. On the other hand, GPGE is a mixed technology providing two energy outputs: renewable electric power from a hot geofluid and fossil energy as natural gas for shipment to a pipeline or for burning on site to generate electricity. As long as both are produced for energy output, such facilities are termed herein as hybrid facilities.

3.1 IGCC

A comparatively new form of electricity production is IGCC. Relative to combustion boiler technologies such as advanced pulverized coal, IGCC is more efficient. The efficiencies for IGCC and its conventional counterparts are 46% and 34%, respectively, for coal feeds, and 40% and 32%, respectively, for biomass feeds (GREET 1.8). The improved efficiency of IGCC is due to dual-stage electricity generation. In the first stage, the fuel is converted to a synthesis gas and subsequently burned in a combustion turbine to generate electricity. In the second stage, the hot exhaust gases from the combustion turbine are directed to a steam generator, which drives a steam turbine to produce additional electricity. At this time, there are only two IGCC plants in operation in the United States: the Wabash River plant, generating 262 MW, and the Polk Power Station, delivering 250 MW. The higher cited operating efficiencies represent plants without carbon capture and sequestration (CCS). Plants with CCS would operate at lower efficiencies.

The materials needed in the largest amounts, by far, for the construction of power plant structures and components (generators, boilers, turbines, and others) are steel and concrete. Though there are other material requirements, like copper, aluminum, plastics, and glass, they are considerably smaller in magnitude in most cases. The steel and concrete requirements for IGCC plants are given in Figures 2 and 3, along with those for other generating technologies. Data values and sources are given in Table A-1. A discussion of life-cycle data for the other generating technologies can be found elsewhere (Sullivan et al., 2010).
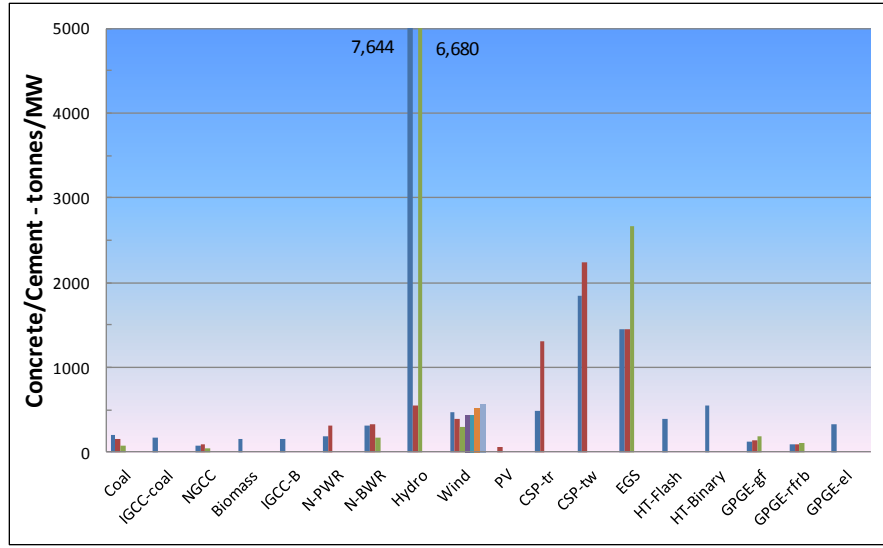
Figure 2 **Concrete/cement requirements of power plants per MW capacity. GPGE data from Argonne modeling, CSP and IGCC data from references given in Table A-1, all other data from Tables 2a, 2b and 2c of Part I.**
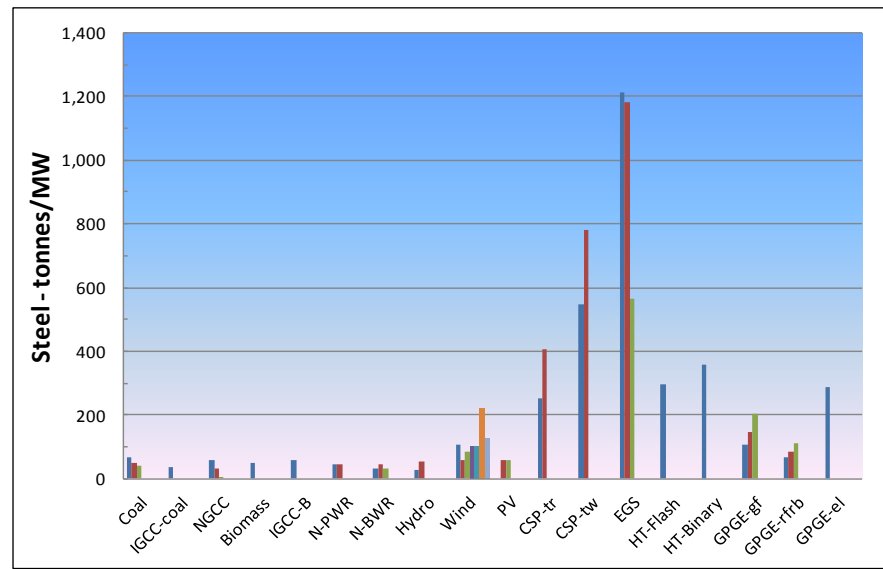
Figure 3 **Steel requirements of power plants per MW capacity. GPGE data from Argonne modeling, CSP and IG CC data from references given in Table A-1, all other data from Tables 2a, 2b and 2c of Part I.**

From an inspection of the figures, the amounts of steel and concrete required to make a MW IGCC power plant are sensibly the same as those for its thermoelectric counterparts,

whether coal- or biomass-fueled. In fact, with the exception of EGS and HT technologies, IGCC MPRs are not markedly different from those of the other thermoelectric plants. However, IGCC plants have componentry differences from standard thermoelectric coal and biomass plants. For example, pulverized coal plants have boilers, while IGCC plants have gasifiers, associated componentry, and another turbine. IGCC plants also operate at higher efficiencies than their conventional counterparts. Despite these differences and the variation in MPRs among plants of the same technology (see discussion in Sullivan et al., 2010), there appears to be a comparable use of steel and concrete between the IGCCs and their conventional counterparts.

Incidentally, additional concrete and steel results not included in Part I are presented in Figures 2 and 3 for pressurized and boiling water nuclear reactors (Peterson et al., 2005). Given the range of MPRs typically observed for any of the technologies, there appear to be no significant differences between the original and newly added results.

3.2   Concentrated Solar Power

The second power-generation technology added to our assessment is CSP. These technologies use reflected radiant energy to heat a heat transfer fluid such as oil to high temperatures, which is generally used to generate steam for driving a steam turbine. The two most mature approaches are the central receiver or power tower (CSP-tw) and the parabolic trough (CSP-tr). For the interested reader, a more detailed discussion of these approaches can be found elsewhere (Viebahn et al., 2008). The CSP-tw technology employs a central receiver upon which light is focused from a surrounding field of mirrors. These mirrors or heliostats track the sun for optimal reflection of radiant energy to the central receiver. Generally, steam is generated to run a turbine generator. However, the temperature at the central receiver can be as high as 1000°C, creating the potential for combined-cycle power generation instead of generation based on the simple steam cycle. Operating fluids include thermo-oil, water (for direct steam), and molten salt.

The other CSP technology covered herein is CSP-tr technology. It employs a field of parabolic (sometimes Fresnel) mirrors, where incident radiant energy is concentrated on a tube of heat transfer fluid running along the trough's focal line. The oil is heated to around 400°C and subsequently used to generate steam to feed a turbine generator. Molten salts can also be used with CSP-tr, especially when thermal storage is employed. When thermal storage is employed at either trough or tower facilities, large amounts of molten salts (nitrates) are stored underground for use in generating power after the sunset or peak demand periods. This capability effectively increases the capacity factor of the facility. Details on the facilities can be found in Table A-1, where references, MPRs, and other plant details are provided. The largest CSP plant in the world is located in California's Mojave Desert and operated by Solar Energy Generating Systems. It is a CSP-tr system, which generates 354 MW.

Though the concrete and steel MPRs for the CSP-tw system are shown in Figures 2 and 3 to be larger than those for the CSP-tr unit, the apparent difference might be due to outdated information. One report (Viebahn et al., 2008) attributes the difference to overdesign of on-site central-receiver buildings and structures, and the other (Koroneous et al., 2008) uses very

outdated central receiver material requirements data from the U.S. Department of Energy (USDOE, 1983). Hence, we treat the MPRs for central-receiver CSP systems as roughly comparable to those for the trough technology, despite the apparent differences shown in the figures.

Further inspection of Figure 2 reveals that the concrete/cement MPRs for both CSP systems are considerably less than those for dam hydro and less than those for EGS, but substantially larger than those for PV, wind, biomass, and HT flash and binary systems. They are also very much larger than those for the conventional systems, such as coal, natural gas, nuclear, and IGCC. The latter observation can be attributed to both the diffuse nature of the energy source (solar) and the material requirements for anchoring into the soil numerous, robust structures of large surface area for concentrating and directing radiant energy.

The steel MPRs for CSP (Figure 3) exceed those for dam hydro, PV, and wind, and are roughly equivalent to those for HT flash and binary, but are less than those for EGS. Owing to the steel and cement requirements for very deep wells (4 to 6 km), it is not surprising that EGS MPRs exceed those for CSP. CSP requires considerably more steel per MW than conventional power systems do. The reason for this is the same as that just given for their concrete MPRs. We pointed out above that the MPRs for CSP systems are much larger than for PV. The choice of support and framing materials for PV can be quite variable. As is evident in Figure 4, aluminum is often used for array framing, and glass and polymeric encapsulating materials provide protection from the weather. In general, comparatively little cement and steel is used for PV array deployment.
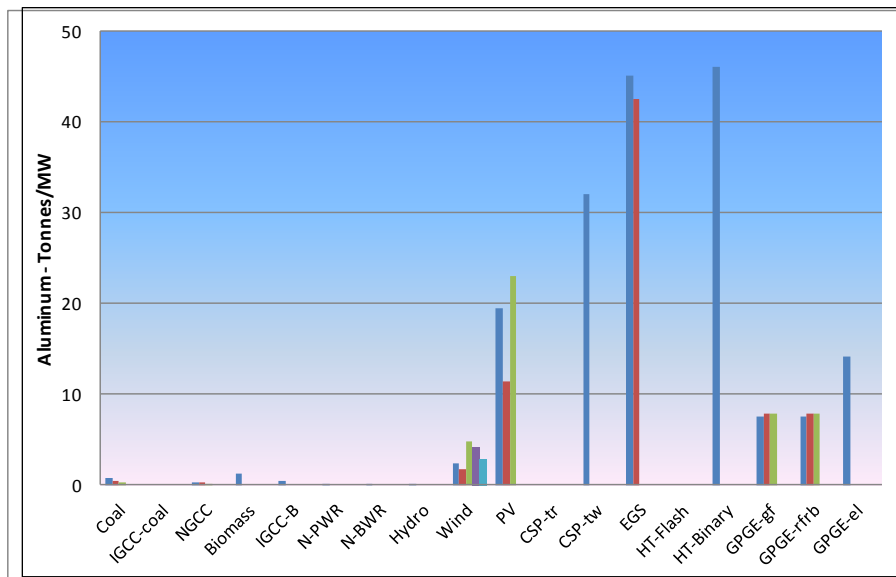
Figure 4 Aluminum use in various power generating technologies. GPGE data from Argonne modeling, CSP and IGCC data from references given in Table A-1, all other data from Tables 2a, 2b and 2c of Part I.

Compared to conventional thermoelectric power production, renewable power plants tend to use considerably more aluminum, as is evident in Figure 4. Its use is quite high for binary geothermal systems, primarily owing to its extensive use for heat exchanging in their air coolers. Though the GPGE systems, which are hybrid facilities, were also assumed to employ air coolers for their binary cycles, the corresponding aluminum MPRs are nonetheless lower than those for their EGS and HT counterparts due to normalization by total system energy output (gas plus electric), MW_{mx}. The aluminum MPR for CSP-tw is higher than those for PV arrays. However, because that CSP value is based on an early-1980s paper cited by Koroneous et al. (2008), it may not reflect modern architectural and construction practice (Viebahn et al., 2008).

3.3   GEO-PRESSURED GAS AND ELECTRIC POWER

Geo-pressured gas and electric plants take advantage of underground pressurized reservoirs that contain both hot water and dissolved natural gas. The resource base includes thermal energy, mechanical energy, and chemical energy (of the methane). As the potentially recoverable mechanical energy is less than 1% of both the thermal and chemical energy (Papadopulos et al., 1975), energy production from GPGE flows has focused primarily on thermal and chemical energy components of the resource (Wallace et al., 1979; Randolph et al., 1992). The dissolved and free (if any) gases are separated from the geofluid prior to directing it through a binary system. The gas is directed to either a gas turbine (or engine) for direct electricity generation or a gas pipeline, while the hot water, after extraction of available thermal energy, is injected back into a reservoir hydraulically isolated from the GPGE reservoir. The first hybrid GPGE plant in the U.S. was the Pleasant Bayou facility, which evaluated the geofluid for electricity production and the natural gas for either electricity production or gas distribution. It is generally thought that the most economically viable approach would be to send the natural gas to transmission pipelines (USDOE, 2010; Randolph et al., 1992). Because most potential GPGE sites overlap with existing gas fields, such locations will already have access to pipelines.

As can be seen in Figure 5, GPGE resources in the U.S. are located primarily in the western states and along both the gulf and pacific coasts. Though the energy potential of GPGE resources is purported to be 160,000 quads (USDOE, 2010), it is likely far less, owing to poor economics resulting from low resource temperatures or a lack of access to the electricity grid. Nonetheless, because some of the sites will certainly be optimally located and have adequate fluid properties, they have the potential to be profitably operated.

Figure 5 GPGE Resources in the U.S. (USDOE, 2010)

We believe that our modeling of the two dual-output GPGE plants spans the range of material needs (MPRs) for such facilities. The GPGE-gf plant should have the greatest material demand (and MPRs), while the GPGE-rfrb should have the minimum. Depending on the amount of well reworking required, the latter could have a material demand as low as a binary plant alone (excluding its wells and above-ground well-to-plant piping). Details on our GPGE scenarios are given in Table 1. Well-field properties assumed for our modeling were taken from USDOE (2010). We also assumed continued coproduction of gas and geofluid over the lifetime of the facility.

Table 1   Parameters Evaluated in GPGE Scenarios

Parameter	Greenfield Site	Reworked Site
Producer to injector ratio	2:1	3:1
Number of turbines	1	1[b]
Generator type	Binary	Binary
Cooling	Air-cooled	Air-cooled
Temperature[a], ^{o}C	130–150	150
Thermal drawdown, % per year	0	0
Well replacement	None	None
Production well depth, km	4, 5, 6	4, 5, 6
Injection well depth, km	2, 2.5, 3	2, 2.5, 3
Gas/brine ratio (SCF/STB)[a]	25–35	34
Flow rate[a], kg/s	35–55	27–47

Table 1 (Cont.)

Parameter	Greenfield Site	Reworked Site
Distance between wells, m	1000	1000
Location of plant relative to wells	Central	Central
Power, MW$_{el}$	(2.8, 3.6, 4.4)[c]	(2.8, 3.6, 4.4)
Gas, 10^6 m^3/yr	(11.1, 14.3, 18.1)[c]	(11.1, 14.3, 18.1)[d]

[a]Based on USDOE, 2010

[b]Could be either 3 small turbines or 1 at 3x capacity

[c]Based on parameters above

[d]Estimated to be the same as the greenfield site

The variants modeled for both GPGE-gf and GPGE-rfrb fields are shown in Table 1. In Figures 2 and 3, three bars are presented for each of these types of facilities. The middle bar represents the midrange facility, which has a 5-km production well, 2.5-km injection well, and power (energy rate) outputs of 3.6 MW$_{el}$ and 17.3 MW$_{th}$. The maximum and minimum bars represent the range of MPRs. The former represent the highest-capacity plants with the shallowest wells and the latter represent the lowest-capacity plants with the deepest wells. For estimating the cement/concrete and steel needs of the binary plant at the GPGE site, the MPRs published in Part I for the binary plant were used. The USDOE's Geothermal Electricity Technology Evaluation Model, GETEM (GETEM, n.d.), was used to estimate well material requirements for the greenfield sites.

An inspection of Figures 2 and 3 reveals that the cement and steel MPRs for GPGE-gf are much lower than those for the EGS and roughly half of those for HT-Flash and HT-Binary power production plants. As per our models, this is primarily because less cement and casing are needed for the smaller bore-hole and casing diameters of geo-pressured wells as opposed to those for EGS wells. Also, the leveraging effect of including natural gas production with generated geothermal electric power reduces the magnitude of GPGE MPRs even further in comparison to other geothermal technologies. (Data for the midrange plants are given in Table A-1.) On the other hand, the MPRs for GPGE-el are about twice those for the GPGE-gf plant. This is due to: a) the extra material needed for the on-site NGCC (natural gas combined cycle) turbine generator and associated structures and equipment and b) the plants' lower overall MW output relative to that of the dual-output plants.

It is expected that reworked wells will be more or less the norm for GPGE systems. At depleted gas wells with existing casings, the main rework is to seal off the old gas zone perforation, perforate the new water zone, and replace the small gas production tubing with large tubing for the higher water flow rate. The amount of new material, mainly the new tubing, is small comparing to the casing of a new well. However, an injection well needs to be drilled for returning cooled water to an underground reservoir other than the production one. Existing disposal wells from previous gas production will not have the capacity needed to handle large

amounts of water. Converting an existing gas well to an injection well may not be an option, owing to the small diameter of the casing in the gas well. Injection wells were again assumed to be about half the depth of production wells, as in the greenfield scenario.

For the modeling of the GPGE-rfrb plant, we assumed the same range of well depths and output capacities as the greenfield sites. For refurbished facilities, we used the same binary plant MPRs as mentioned above for the power plant; for the wells, one injection and three production strings were employed. We noticed that three productions wells produced about the same amount of geofluid as two production wells in the greenfield scenario. The steel and cement/concrete MPRs for this plant are also shown in Figures 2 and 3 (also see Table A-1 for midrange values). As expected, reworked plants have lower steel and cement/concrete MPRs, which are primarily attributed to existing wells with intact casings. Note in Figures 2 and 3 that the highest MPRs for a refurbished site are on par with those of the lowest greenfield site. In fact, on the basis of the midrange bars, the refurbished plant requires about two thirds of the steel and concrete/cement of a greenfield site.

An inspection of Figure 6 reveals that across power technologies, the total mass of materials required for building power plants more or less mirrors the above trends in steel and concrete MPRs. The trends are the same as previously reported (Sullivan et al., 2010). PV shows the lowest overall materials demand of any of the renewable technologies, with the possible exception of biomass power. Notice that CSP plants show about the same total MPRs as EGS plants, even though EGS plants had greater steel and concrete MPRs. The reason for this is the large amount of nitrate salts used for thermal storage at CSP facilities.
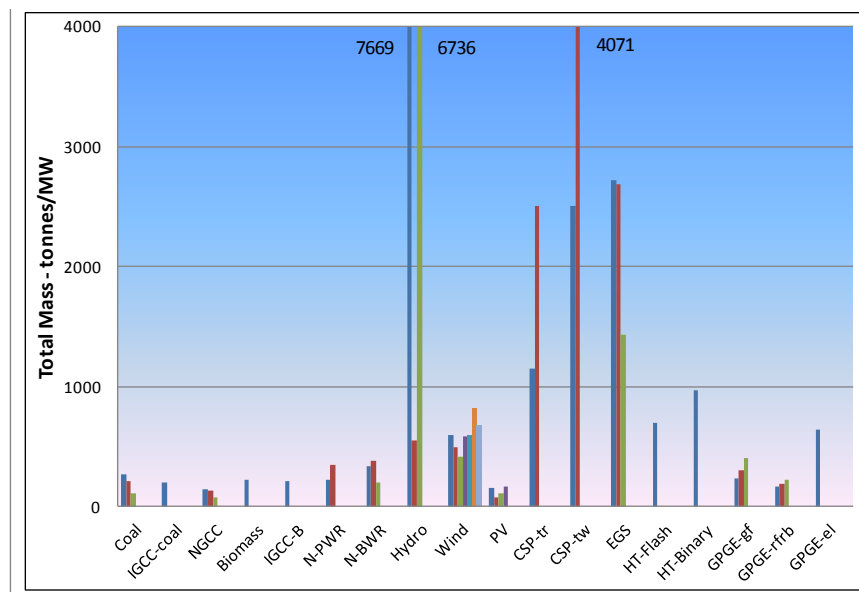
Figure 6   Total mass of materials required for various power generating technologies: GPGE data from Argonne modeling, CSP and IGCC data from references given in Table A-1, all other data from Tables 2a, 2b and 2c of Part I.

13

4 WELLS

In this section, we describe the well-field modeling assumptions for our GPGE scenarios. We also discuss and characterize well-field material and fuel requirements as a function of well depth for all of the geothermal systems analyzed, including EGS, HT-Flash, and HT-Binary, and GPGE systems. Finally, the impact of exploration activity on well-field development is also discussed in detail.

4.1 GPGE WELLS—GREENFIELD SITE

This section describes the assumptions used to model a geo-pressured greenfield site. Table 1 shows the scenarios across several design parameters, which affect performance, cost, and environmental impacts. The scenarios were modeled in GETEM, and the simulation was run multiple times in GETEM to create a range of possible outcomes. A detailed discussion of well-modeling methodology can be found elsewhere (Sullivan et al., 2010). In the discussions that follow on coproduced systems, only departures from the assumptions employed previously are covered.

4.1.1 Well-field Development

It was assumed that the production wells would be twice the length of the injection wells, according to well configurations at Pleasant Bayou (Randolph et al., 1992). The components included in the inventory for each well are depicted in Figures 7 and 8, and characteristics of production and injection well components are given in Tables 2 and 3, respectively.

The major differences between a geo-pressured well and a traditional geothermal well are the completion method and the use of production tubing. Most of the EGS and HT wells use open-hole completion, where a slotted liner is placed at the production/injection zone without perforation. A geo-pressured well has overpressured gas in the production fluid, and fluid contamination between rock formations is a concern. Therefore, cased hole completion and perforation are needed for a geo-pressured well, just like a normal oil/gas well. For the same reason, as well as because of government regulations, production tubing must be used in geo-pressured wells. However, the production tubing needs to have a larger diameter than that commonly used in an oil/gas well, for higher flow rate.

4.1.2 Drilling: Fuel and Fluids

To determine the amount of fuel consumption per day required for drilling for each of the six well depths (2, 2.5, 3, 4, 5, and 6 km), data from the previous study were graphed, with well depth, in km, on the x-axis and drill rate, in m/day, on the y-axis. The data for wells less than or equal to 3 km in depth appeared to lend itself to a linear line of best fit, while the data for those greater than 3 km appeared to be best fit by a logarithmic function. With the functions

approximating drill rate as a function of well depth, the drill rate could be calculated for each of the six well depths listed in Table 1. From drill rate and depth, the duration of drilling could be estimated.

For this study, we assumed that a 2,000-hp rig was required for the production well and a 1,000 hp-rig for the injection well. These two rigs consume 1,296 and 648 gallons of diesel per day, respectively.

4.1.3   Well Casing

The casing materials required for our production and injection wells are listed in Tables 2 and 3, respectively. For reworked well designs, it was assumed that only the production tubing in the abandoned wells requires replacing. For reworked wells, a 3:1 ratio of production to injection wells was assumed.
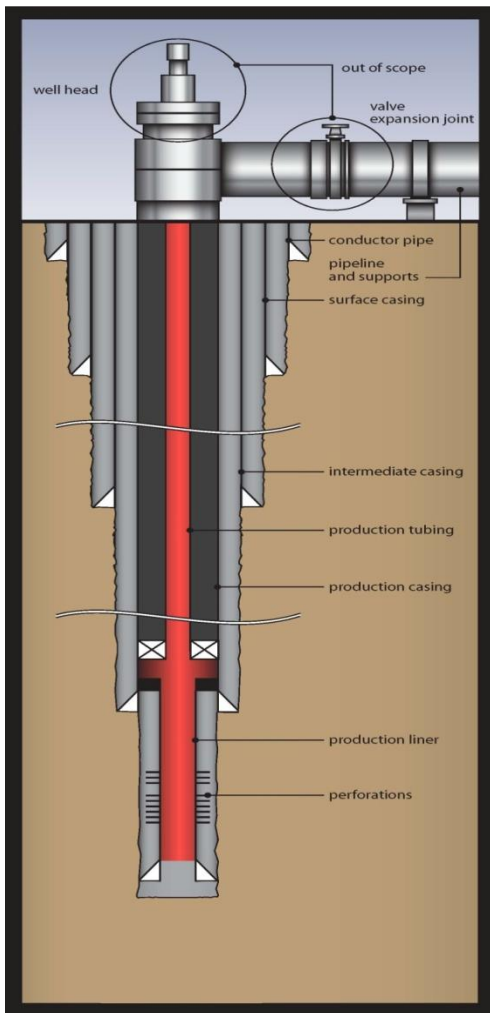
Figure 7   Production Well Design   **Figure 8   Injection Well Design**
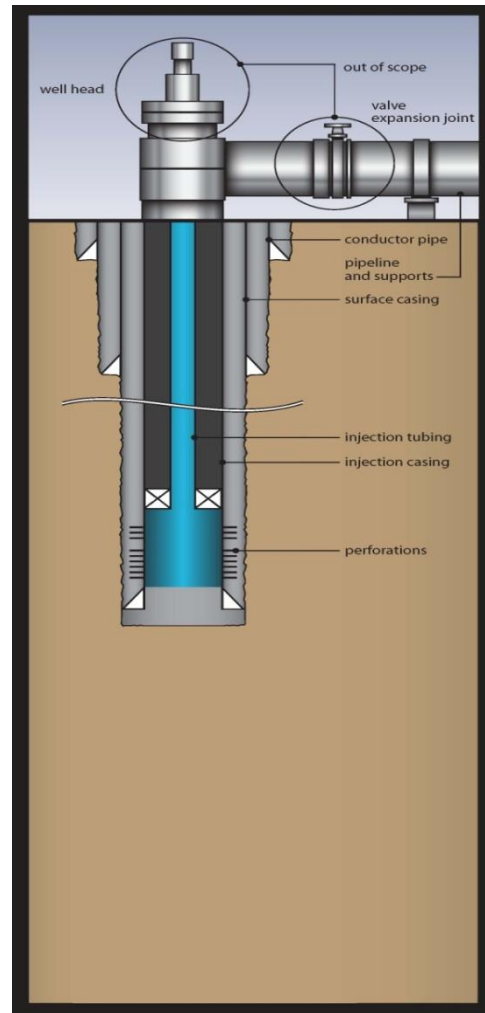
Table 2   Production-well Component Characteristics at the Considered Depths, Based on GETEM

Well Depth (km)	Casing Schedule	Material	Depth (m)	Hole diam (cm)	Casing diam (cm)	Weight/Length (kg/m)
4	Conductor pipe	Welded wall	31	76.20	66.04	202.64
	Surface casing	H-40 and K-55 casing	338	60.96	50.80	139.89
	Intermediate casing	S-95, L-80, and N-80 casing	2,058	44.45	33.97	107.15
	Production casing	S-105, S-95, and S-105 buttress	3,463	31.12	24.45	79.62 (69.94 for S-95)
	Production liner	P-110 SHFJ liner	3,992	21.59	17.78	56.55
	Production tubing	P-110 tubing	3295		13.97	25.35
5	Conductor pipe	Welded wall	38	76.20	66.04	202.64
	Surface casing	H-40 and K-55 casing	423	60.96	50.80	139.89
	Intermediate casing	S-95, L-80, and N-80 casing	2,572	44.45	33.99	107.15
	Production casing	S-105, S-95, and S-105 buttress	4,329	31.12	24.46	79.62 (69.94 for S-95)
	Production liner	P-110 SHFJ liner	4,989	21.59	17.78	56.55
	Production tubing	P-110 tubing	4,119		13.97	25.35
6	Conductor pipe	Welded wall	46	76.20	66.04	202.64
	Surface casing	H-40 and K-55 casing	507	60.96	50.80	139.89
	Intermediate casing	S-95, L-80, and N-80 casing	3,086	44.45	33.99	107.15
	Production casing	S-105, S-95, and S-105 buttress	5,194	31.12	24.46	79.62 (69.94 for S-95)
	Production liner	P-110 SHFJ liner	5,987	21.59	17.78	56.55
	Production tubing	P-110 tubing	4,943		13.97	25.35

Table 3   Injection-well Component Characteristics at the Considered Depths, Based on GETEM

Well Depth (km)	Casing Schedule	Material	Depth (m)	Hole diam, (cm)	Casing diam, (cm)	Weight/Length (kg/m)
2	Conductor pipe	Welded wall	20	76.20	66.04	202.39
	Surface casing	H-40 and K-55 STC casing	396	60.96	50.80	139.89
	Injection casing	S-95, N-80 SSTC, and buttress casing	2,000	44.45	33.99	107.15
	Buttress	N-80 buttress casing	1,832	33.97	24.46	59.53
	Injection tubing	K-55 and J-55 tubing	1,751	-	13.97	23.07
2.5	Conductor pipe	Welded wall	25	76.20	66.04	202.39
	Surface casing	H-40 and K-55 STC casing	495	60.96	50.80	139.89
	Injection casing	S-95, N-80 SSTC, and buttress casing	2,500	44.45	33.99	107.15
	Buttress	N-80 buttress casing	2,289	33.97	24.46	59.53
	Injection tubing	K-55 and J-55 tubing	2,188	-	13.97	23.07
3	Conductor pipe	Welded wall	30	76.20	66.04	202.39
	Surface casing	H-40 and K-55 STC casing	593	60.96	50.80	139.89
	Injection casing	S-95, N-80 SSTC, and buttress casing	3,000	44.45	33.99	107.15
	Buttress	N-80 buttress casing	2,747	33.97	24.46	59.53
	Injection tubing	K-55 and J-55	2,626	-	13.97	23.07

4.1.4   Cementing of Casing

The volume of cement needed for each well was determined by calculating the total volume of the well and the volumes of the casing and interior, and accounting for excess cement for each casing interval. In the Pleasant Bayou GPGE well, Class H cement was used (Randolph et al., 1992). Typically, Class G cement is used in California, the Rocky Mountains, and Alaska, while Class H cement is used in most other places in the world, including along the coast of the Gulf of Mexico (Gulf Coast), where Pleasant Bayou is located. As GPGE resources exist in various geographic regions within the U.S., including the Gulf Coast and California (USDOE, 2010), calculations were conducted with both Class G and Class H cement and accounted for different material usages. Classes G and H cement with no silica flour were used for the conductor pipe and surface casing, while Classes G and H with 40% silica flour were used for the rest of the casing cement. Silica flour is an additive that is often used to enhance cements for high-temperature applications (Bourgoyne, 1991, p. 102). With the corresponding estimated

volumes of water (gal/sack) and slurry (ft^3/sack) (see Table 4), it was possible to estimate the water used in cementing the casing.

Table 4   A Comparison of Class G and Class H Cement

	Class G		Class H	
% Silica flour	0	40	0	40
Water volume (gal/sack)	5	6.8	4.3	5.99
Slurry volume (cu. ft/sack)	1.15	1.62	1.06	1.51

Owing to its small production energy and small contribution to $\mathcal{E}_{pc}$ and GHG_{pc}, which are estimated later in this report, we have not included silica flour in the cement weight. However, for the interested reader, the amounts of silica flour can be readily estimated from the following expression of the cement to silica flour ratio:

$$Cement/Si\_flour \ = \ 9.03 * Exp\,[\text{-}1.2 * depth] + 2.9$$

This empirical expression is a first approximation of silica flour requirements for wells as a function of well depth (in km) and applies to EGS, HT, and GPGE wells.

4.1.5   Pipelines between Wells and Plant

For this study, it was assumed for the greenfield site that each of two production wells has a separate pipeline to deliver the hot geofluid to the power plant and a final pipeline to carry the cooled geofluid to the injection well from the power plant. This study assumes two production wells and one injection well per geothermal power plant. As the pipelines are aboveground, they require both support structure and insulation. The associated steel, water, cement, and diesel usages for these pipelines have been accounted for.

4.1.6   Pipeline

Assuming a minimal pressure drop of 10 psi (68.95 kPa) across the entire length of pipeline and pipeline lengths of 600, 800, 1000, 1200, 1400, and 1600 m, pipe diameters were calculated as before. A range of temperature values (130–150°C) and a range of mass flow rates (35–55 kg/s) were considered (see Table 1).

Using the above parameters, the maximum diameter was calculated to be less than 8 in. Each scenario above was also run with twice the mass flow rate to account for the pipeline leaving the plant and delivering geofluid to the injection well as it manages the flow of both of the production wells. The maximum diameter obtained for the injection pipeline was found to be

less than 10 inches. The two pipe diameters determined here, 8 in. and 10 in., are consistent with the diameters of the production and injection pipelines used in the Pleasant Bayou GPGE plant. The Pleasant Bayou production pipe diameters were 7 in. and the injection pipeline diameter was 8 in., as described by Randolph et al. (1992). For our analysis, schedule 40 steel pipe was assumed for a weight per length of 28.55 lb/ft (42.49 kg/m) for the 8-in-diam pipe and 40.48 lb/ft (60.24 kg/m) for the 10-in-diam pipe.

4.1.7   Pipeline Supports

The material requirements for the pipeline support system include forming tubes (sonotube boards), concrete, and rebar for the foundation, and steel for the structural support. Insulation was used at support contacts as well as along the length of pipe from the production well to the power plant. The design for the foundation is the same as the one described by Sullivan et al. (2010). The recipe assumed for this analysis is for controlled low-strength material concrete and assumes 125 pounds of Portland cement, 2,500 pounds of fine aggregate, and 35– 50 gal of water (IDOT, 2007). Given the diameter (15.75 in) and depth (6 ft) of each hole, one can calculate the volume of the hole. The volume of concrete required is the hole volume minus the volume taken up by the 12-in-long, 0.5-in-diam rebar.

4.1.8   Pipeline Insulation

Insulation was estimated to weigh 4 lb/ft (6 kg/m) in 3-ft (0.94-m) lengths (Knauf Insulation GmBH, 2008). It was assumed that one 3-ft section was wrapped around the injection pipeline at each support while both production pipelines were covered in insulation along their entire lengths.

4.2   GEO-PRESSURED WELL: REFURBISHED WELLS

Relative to the greenfield cases discussed above, there are many possible variations in materials and fuel demand for refurbished wells, depending on the specific conditions of existing gas fields. Because the major cost of field development is drilling, a practical approach is to take advantage of existing gas wells that 1) are deep enough to penetrate the geo-pressured reservoir; 2) have sufficiently large-diameter hole and casing to support a high water flow rate; and 3) have reached the end of their cost-effective gas production lifetime. Our assumptions for refurbished wells and production output are given in Table 1. These numbers are mostly provided by the Universal GeoPower project, which is partially supported by the USDOE (Luchini, 2011). These wells can be reworked in order to produce both hot brine and gas from a GPGE resource. The rework includes mainly sealing (cementing) off the old gas zone perforation, perforating the geo-pressured water zone(s) and replacing the small-diameter gas production tubing with a larger-diameter tubing for brine production (see Table 5 for details).

Table 5   Existing Casing and New Tubing Dimensions for Production Wells

Well Depth (km)	Casing Schedule	Material	Depth (m)	Casing/Tubing diam (cm)	Weight/Length (kg/m)
4	Production casing	Various	4000	15–18	existing
	Production tubing	P-110	3500	13.97	25.3
5	Production casing	Various	5000	15–18	existing
	Production tubing	P-110	4500	13.97	25.3
6	Production casing	Various	6000	15–18	existing
	Production tubing	P-110	5500	13.97	25.3

A well for re-injecting wastewater to a reservoir that is hydraulically isolated from the production zone may need to be drilled. Existing injection wells, if there are any near the site, will not be able to handle the large amount of brine being produced from multiple production wells. Existing gas production wells are usually too small to be converted to an injection well. The ratio between production and injection wells is likely to change from field to field. For our model, we assume a 3-to-1 ratio, as the reworked production well may not generate as much flow as a new well. To represent these injection wells, we use their greenfield counterparts. (For dimensions of well casing and tubing stock, see Table 3.)

The possible surface facilities can vary, depending on the local conditions. For example, if the soil is thick, pipeline can be buried economically without extra supporting structure. However, this approach will not be practical for a rocky terrain. In addition, one generator for three production wells may be more efficient, while one small generator for each well may reduce the startup cost and risk. In this rework scenario, we assume one small generator for each well so that no pipe or insulation is needed for hot water. Furthermore, the wastewater pipeline can be buried, so that no supporting system is needed.

4.3   UPDATED AND EXPANDED GEOTHERMAL POWER DATA

In our previous report (Sullivan et al., 2010), we included well materials in our analysis of three geothermal technologies, namely, EGS, HT-Flash, and HT-Binary. However, because only aggregate values were reported, materials burdens for the wells themselves were not evident. Further, materials required for well exploration were also not itemized. Finally, additional information on plant construction has also been developed and is presented below.

4.3.1   Well Material Requirements

Figures 9-11 show the cement, casing (steel), and diesel fuel demand per MW of plant capacity as a function of well depth. Water requirements for drilling these wells can be found in a separate report (Clark et al., 2011a). The data in the figures can readily be converted to a per-well basis using the factors found in Table 6. The results in the figures represent material and

fuel requirements as a function of depth for six well configurations: 1) the comparatively shallow wells for the HT-Binary plant, 2) the intermediate-depth wells of the HT-Flash plant, 3) three variants of deep EGS wells, and 4) geo-pressured wells at a greenfield site.

Figure 9   **Cement demand vs. well depth for five well cases: for data with range bars that obscure each other, ±0.05 km has been added to the depths of overlapping pairs to facilitate comparison.**

There are some features in the figures that merit comment. Notice the jumps in steel and cement demand at 2 and 5 km for the HT-Flash well and at 6 km for the EGS well. These jumps are due to the need for intermediate casings for geothermal wells of greater depths. In general, because of the need to isolate groundwater from source fluid and limitations on a drilling rig's load-bearing capacity to support a casing string, a deeper well will have a greater number of casing strings, each with a smaller diameter than the one above it (see Tables 3a and 3b in Sullivan et al., 2010). Further, EGS wells have to be large and robust enough to accommodate in-line pumps and the pressures required for well stimulation to hydraulically open existing fractures in the resource rock for enhancing geofluid flow and heat exchange. This requirement is particularly evident for the EGS facilities shown in the figures, where the data points for 1, 2, and 3 intermediate liners appear to correspond to progressively greater cement and steel (casing) demand trend lines.

**Figure 10   Steel requirements vs. depth for five well cases:
for data with range bars that obscure each other,
±0.05 km has been added to the depths of
overlapping pairs to facilitate comparison.**

On the other hand, considerably less cement and steel are evident in Figures 9 and 10 for a MW of GPGE output. The reasons are twofold: 1) smaller-diameter casings characteristic of gas wells, and 2) the leveraging effect of two coproduced energy products. Because these are artesian wells with significant pressures, there is no need for the larger-diameter casings to accommodate line pumps as is the case for EGS wells.

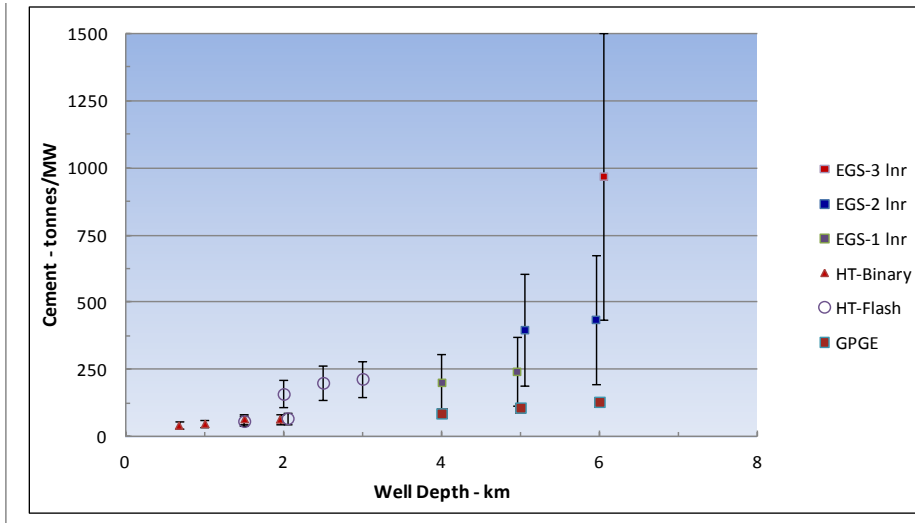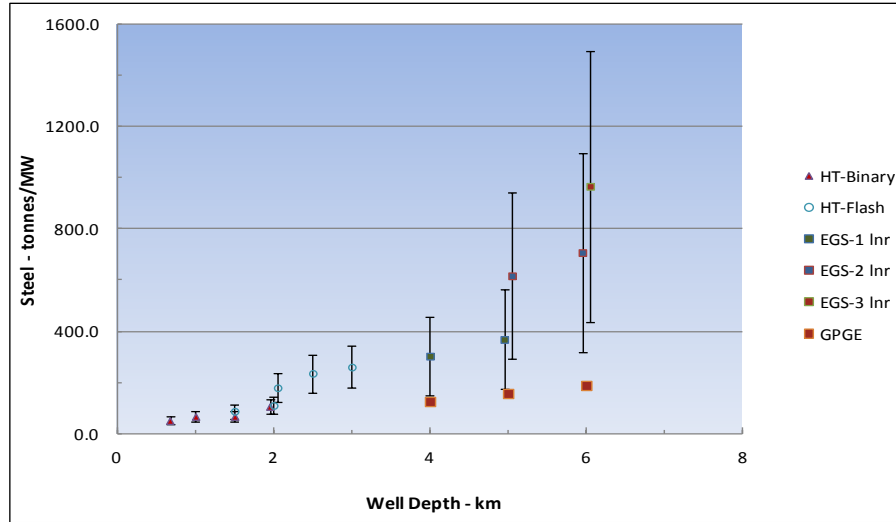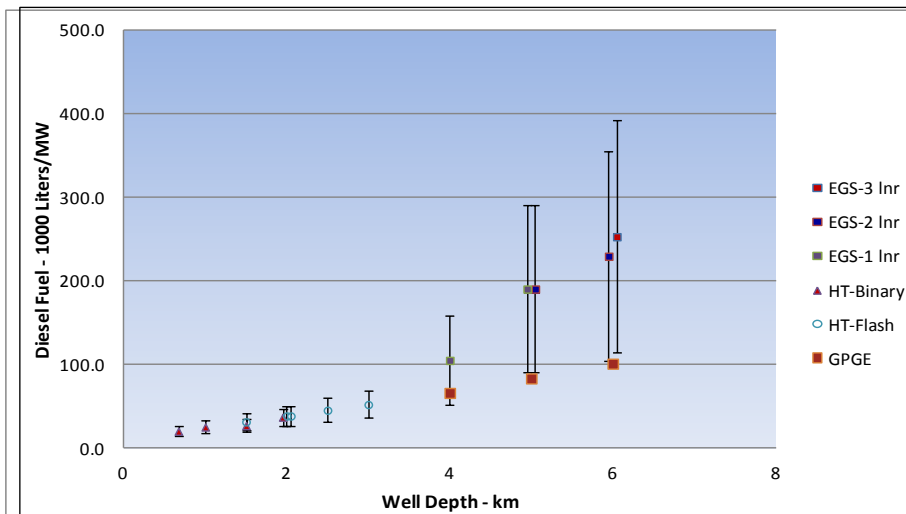**Figure 11   Diesel fuel requirements vs. depth for five well cases:
for data with range bars that obscure each other,
±0.05 km has been added to the depths of overlapping
pairs to facilitate comparison.**

22

Another feature to be noted in Figures 9 and 10 is the comparatively wide range of results associated with each data point. This width is due to variations in modeling assumptions concerning source temperatures and well flow rates (see Table 6).

As seen in Figure 11, while demonstrating the same variation in range at each depth, the diesel requirement for the various wells does not appear to show the same step changes at certain depths observed in the data for steel and cement. Though the initial trend appears to be linear with depth up to 3 km, the trends become non-linear thereafter for EGS plants. The reason is that at progressively greater depths, more casing strings are needed, requiring drilling rigs of progressively higher horsepower to manage increased string weight. When the initial linear trend is extended to 4 to 6 km, it appears co-linear with the diesel requirements for drilling greenfield GPGE wells. This finding is consistent with the lower casing demand and smaller tubing diameters required for GPGE field exploitation.

Table 6   Modeling Variation Assumed for Various Geothermal Plants (see Table 1 for GPGE Plants)

Plant	Depth (km)	T_{source} (^{o}C)	Flow Rate (kg/s)	<wells/MW>[a]	Plant Capacity (MW)
HT-Binary[b,c]	0.7, 1, 1.5, 2	150, 165, 185	60, 90, 120	0.42	10
HT-Flash[b,c]	1.5, 2.5, 3	175, 200, 250, 300	40, 60, 80, 100	0.41	50
EGS[b]	4, 5, 6	150, 175, 200, 225	30, 60, 90	0.48	20 & 50

[a]Average

[b]Based on Raft River well configurations.

[c]Applies to both production and injection wells.

In summary, cement and steel requirements for geothermal wells appear sensibly linear to depths up to 2 km, but depart significantly from linearity with increasing depth as the need increases for multiple strings of different-diameter casing. The only exceptions are GPGE wells, where materials requirements appear collinear with shallower geothermal-well trend lines. Similar observations are evident for the diesel fuel required to drill wells.

4.3.2   Exploration Wells

Because drilling production and injection wells at a potential geothermal site is an expensive undertaking, a geothermal developer must be convinced that a viable fluid resource is present before starting. A number of geological, geochemical (CO_2 and Hg concentrations of fluids, elemental and isotopic ratios, temperature gradients) and geophysical (magnetics, resistivity, gravity and seismicity) methods can be employed to establish whether a potential geothermal resource is present. A brief discussion of these approaches can be found elsewhere (Jennejohn, 2009). If the results from these test methods are sufficiently encouraging, a decision

is made to drill exploratory wells. However, there is little published information on the number of such wells needed to confirm the viability of the geofluid resource. These wells are generally smaller than production wells. Our modeling assumed that exploration wells have the same material requirements as production wells, which in turn were assumed to have the same material needs as injection wells Although exploration wells are typically lower in material and fuel demand than production and injection wells, assuming equivalence provides a conservative estimate of exploratory well burden, especially given the uncertainty about the number of such wells needed to confirm a site's resource potential. Hence, our exploration wells are equivalent to a production well.

Given the above, we can estimate the incremental cement, steel, fuel, and water (see water data in Clark et al., 2011b) required for the exploration well activity. For the 10-MW HT-Binary system, the incremental cement, steel, and diesel fuel is about 22% of the existing burden for the production and injection wells. On the other hand, for the HT-Flash plant, the incremental burden is around 4.5%. The reason for the distinct difference between the two plants is related to plant capacity. As capacity increases, the greater is the number of wells required to support it, though the number of exploration wells in both cases was assumed to be one. In our modeling, the ratio of exploration to production/injection wells was 1:4.1 for the HT-Binary plant, whereas it was 1:20.6 for the HT-Flash plant.

EGS plants can require 4- to 6-km-deep wells, which are much more expensive to drill than HT-Flash and HT-Binary plants. Hence, to minimize financial risk, a thorough and complete exploration and assessment of the geothermal site is called for. After satisfactory completion of geochemical and geophysical surveys, some combination of thermal gradient holes and slim holes are drilled to establish whether the potential geothermal resource is hot enough for commercial application. Unfortunately, there is little publicly available information on the extent of such drilling and its site-to-site variation. What is certain is that slim holes can be expensive, depending on depth. Given this uncertainty, we applied the same rule mentioned above to the HT systems, namely, the exploration drilling activity is approximated as the materials and fuel required for drilling additional production wells. This equivalence was assumed for our 20-MW EGS system, i.e., the drilling of exploration wells adds 10.5% to well cement, casing, and fuel requirements. Because the 50-MW EGS plant is so much larger than a 20-MW facility, two wells are added to the total number of production and injection wells, amounting to an additional 4.2% of cement, casing, and diesel fuel.

5   SERVICE FUNCTIONAL UNITS $\mathcal{E}_{pc}$ AND GHG$_{pc}$

In this section, we compute $\mathcal{E}_{pc}$ and GHG$_{pc}$, two important metrics used for characterizing and comparing the life-cycle performance among the power-generating systems discussed herein and previously (Sullivan et al., 2010).

5.1   PLANT CONSTRUCTION

As pointed out above, the original report considered only indirect burdens in estimating plant cycle burdens. The energy that indirect burdens represent is primarily the burdens incurred in producing the materials that comprise facilities. Omitted from that plant cycle estimate were the direct burdens, which are incurred during the on-site construction activities (energy for earth moving , running cranes and other equipment) and energy expended in transporting materials to the site. The availability of construction life-cycle data is extremely limited. However, construction data are available for a number of other structures, including a university building, office buildings, and residences. The percentage of E_{pc} that is direct energy consumption was reported to be about 4% for residences (Blanchard et al., 1998), assumed to be about 5% for a 5-story academic building (Scheuer et al., 2003), and estimated to be about 12−13% for a 3-story office building, both with and without underground parking (Cole and Kernan, 1996). The latter study included wood-, steel-, and concrete-framed structures. Cole (1999) later estimated the direct energy percentages of the E_{pc} for just the structural systems of buildings, finding 6.0−16% for wood frames, 2−5% for steel frames, and 11–25% for concrete frames. Note that these percentages, which pertain only to building structures, can be higher than those for entire buildings. However, building construction entails more than just structure; also included are site work, envelope, finishes, and services.

Unfortunately, life-cycle construction information for power plants is not available. Hence, to estimate the impact of direct energy on our E_{pc} values, we have taken a conservative approach and assumed that the power-plant direct energy component is 12% of E_{pc}. This value, taken from the 3-story building study, is one of the highest values listed above. However, this value needs adjusting because it includes worker transportation. Cole (1999) reported that 28% of the direct energy consumption is for on-site activities, 43% is for worker transportation, and 29% is for transportation of materials and supplies to the site. Because worker transportation is outside of our system boundaries (and those of most other LCAs), we consider only on-site activities and materials transportation. Hence, the direct energy component is reduced from 12% to 6.8% of E_{pc}, with 25% of the direct component going to electricity and 75% to diesel fuel. With these fuels added to our previous materials and energy list for each of the plants studied, our previously reported values (Sullivan et al., 2010) of $\mathcal{E}_{pc}$ for the various power plants increase by around 7%. For example, previously reported values of $\mathcal{E}_{pc}$ and GHG$_{pc}$ for one of our conventional coal plants were 0.00259 and 0.869, respectively. They are now 0.00279 and 0.924, respectively. For construction of geothermal sites, the above-mentioned estimates were applied only to the construction of topside structures. The construction activity for drilling wells had already been accounted for.

As just indicated, accounting for direct energy consumption and associated emissions during facility construction amounts to a small fraction of $\mathcal{E}_{pc}$ and $GHG_{pc.}$ Going even further back into the life cycles of the power generating systems (e.g., energy and emissions to make the factories that produce plant materials) is unnecessary and will not sensibly improve estimates of their energy and emissions performance.

5.2   VALUES FOR $\mathcal{E}_{PC}$ AND GHG_{PC}

Based on the MPRs discussed above, our calculated $\mathcal{E}_{pc}$ and GHG_{pc} values for the additional power systems, shown in Figures 12 and 13, respectively, are similar to previous results. Values can be found in Table A-2. Emissions, GHG emission factors, and fuels required for plant material production were taken from GREET 1.8 and GREET 2.7. Several features of these figures merit comment.
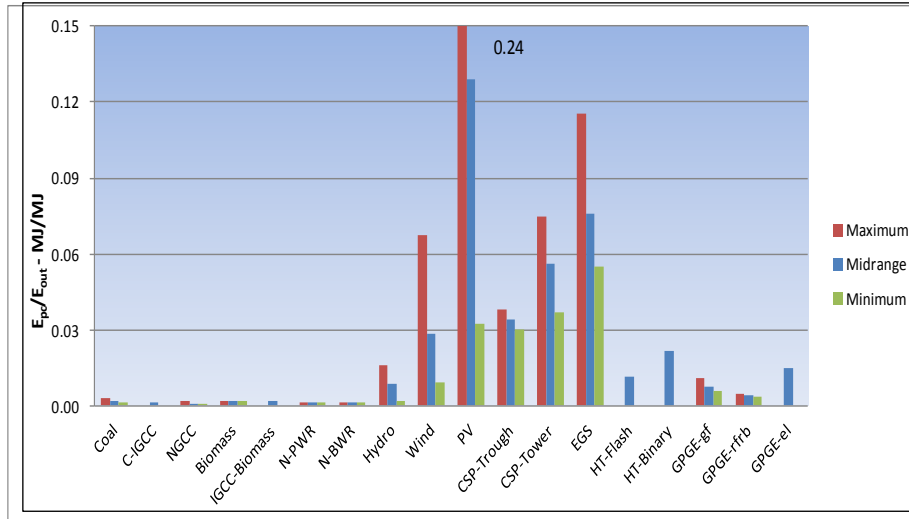
Figure 12   Plant cycle energy ($\mathcal{E}_{pc}$) for various power production technologies relative to total energy output: GPGE data from Argonne modeling, CSP and IGCC data from references given in Table A-1, all other data from Tables 2a, 2b and 2c of Part I.

First, for IGCC power, whether derived from coal or biomass, $\mathcal{E}_{pc}$ values are sensibly the same as those for other conventional thermoelectric plants. This is fully consistent with our previous observation (Sullivan et al., 2010) that for conventional thermoelectric plants (coal, gas, nuclear, biomass), $\mathcal{E}_{pc}$ typically ranges between 0.001 and 0.003. Accordingly, GHG_{pc} values for the IGCC are also consistent with previous values, ranging from 0.3 to 1.1 g/kWh. Also notice that $\mathcal{E}_{pc}$ and GHG_{pc} values for CSP technologies are lower than those for their PV counterparts, despite the fact that just the reverse was true for their respective steel and concrete MPRs. There are two reasons for this. First, CSP facilities have thermal storage, which relative to PV facilities significantly increases their capacity factors thus reducing their $\mathcal{E}_{pc}$ and GHG_{pc} values. On the

other hand, PV facilities use a lot of silicon, which has a high production energy thus increasing their $\mathcal{E}_{pc}$ and GHG_{pc} values.

Also notice that $\mathcal{E}_{pc}$ and GHG_{pc} values for the dual-output GPGE plants are half or less of those for HT-Flash and HT-Binary plants. This is consistent with their steel and concrete/cement MPRs. However, given that the GPGE plants have binary power technology topside and their wells are deeper than those of the binary and flash plants, one might expect that their $\mathcal{E}_{pc}$ and GHG_{pc} values would be lower. The reason they are not lower is the same as that for their MPR trends vs. those for HT flash and binary, i.e., the leveraging effect of two energy products per facility for dual-output GPGE plants. The sets of bars shown in the figures for GPGE-gf and GPGE-rfrb plants represent the following range: deepest wells with lowest output, shallowest wells with highest output, and finally median well depth with median output. (See Table 1 for details.) Finally, notice that the GPGE-el plant, unlike its dual-output counterparts, has $\mathcal{E}_{pc}$ and GHG_{pc} values comparable to those of the HT-Flash and HT-Binary plants. This observation is due to the GPGE-el plant's additional material requirements for its combustion turbine system and lower total output energy.
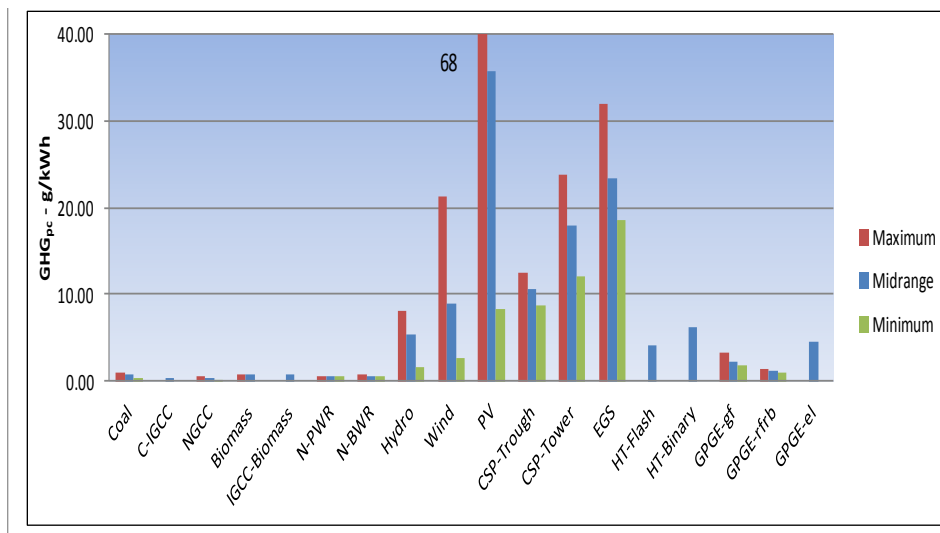
Figure 13   Plant cycle greenhouse gas emissions for various power generating technologies relative to total energy output: GPGE data from Argonne modeling, CSP and IGCC data from references given in Table A-1, all other data from Tables 2a, 2b and 2c of Part I.

With the exception of biomass-based power, the figures show that both the renewable and hybrid technologies have higher $\mathcal{E}_{pc}$ and GHG_{pc} plant cycle values than their conventional thermal electric counterparts.

The impact of well depth on GPGE $\mathcal{E}_{pc}$ and GHG_{pc} can be significant. A plot illustrating this dependency is shown in Figure 14 for GHG_{pc}. The lines shown in the figure are intended only to separate the two groups of geothermal facilities. The GHG_{pc} values for EGS and HT-

Binary increase with well depth and appear to belong to the same trend. Two values each at 5 and 6 km for EGS simply denote wells with one and two liners and with two and three liners, respectively, thus illustrating the impact of increased well materials on GHG_{pc} at a fixed depth. On the other hand, the trend at the bottom of the figure shows that HT-Flash and GPGE require considerably less material per unit energy output. At comparable depth, the material requirements for HT-Binary are shown in the figure to be considerably higher than those for HT-Flash, a fact due to the significant amounts of steel, concrete, and aluminum required for constructing their air cooling systems. However, GPGE facilities were also assumed to use air cooling systems and they do not demonstrate the GHG_{pc} values of EGS and HT-Flash. This finding is a result of two factors: 1) the dual output of the GPGE and 2) less material-intensive wells.
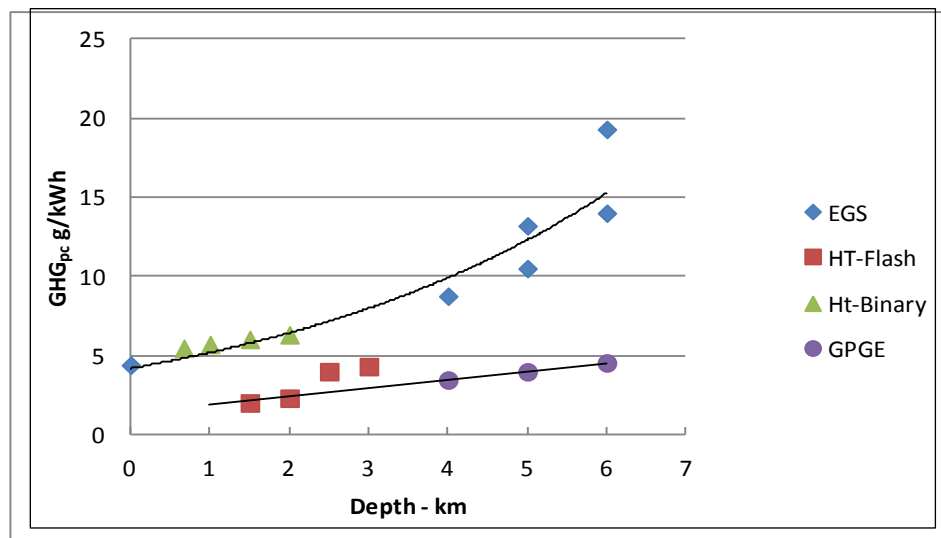
Figure 14   Influence of Well Depth on GHG_{pc} for Geothermal Technologies

Instead of sending produced natural gas to a pipeline, the GPGE-el plant burns it on site to produce additional electricity, which is then sent to the grid. Assuming a greenfield GPGE site employing an onsite NGCC combustion generator with an operating efficiency of 46% (GREET 1.8), we calculated this system's $\mathcal{E}_{pc}$ and GHG_{pc} values to be 0.0221 and 6.65 g/kWh, respectively, for comparable geofluid flows and wells corresponding to the midrange GPGE-gf scenario given in Section 3.3. When compared to the midrange results in Table A-2 for the greenfield site, these values are seen to be about a factor of 1.7 as high. The reasons for this are: 1) lower output capacity (7.5 MW_{el}) for the all-electric plant vs. 12.3 MW_{th} for the mixed-output facility, and 2) additional materials, over and above those already in the mixed-output plant, needed for the NGCC set for combustion of natural gas to electricity. Factor 1 is by far the dominant contributor to the difference.

5.3   GHG EMISSIONS FROM U.S. GEOTHERMAL FACILITIES

During operation, there are GHG emitted from some geothermal facilities. Though in principle binary plants emit zero GHGs, finite and sometimes significant GHGs are released from flash plants, which represent the largest fraction of the geothermal plant population. For flash plants, the geofluid is exposed to the atmosphere during operation resulting in carbon dioxide releases. Bloomfield et al. (2003) reported a weighted average of 91 g/kWh from U.S. geothermal power plants. Their average includes the zero GHG emissions from binary plants, which represent 14% of the surveyed capacity. When adjusted for flash plants only, their average becomes 106 g/kWh. Unfortunately, no mention of the range of U.S. geothermal emissions rates was given by Bloomfield et al. (2003). Their results are based on a study wherein, by agreement with geothermal plant operators, individual sources and values for provided emission rates remain confidential.

A comprehensive global survey of GHG emissions from geothermal power plants was conducted by Bertani & Thain (2001) . Their data, shown in Figure 15, ranges from 4 to 740 g/kWh and represents 85% of global capacity, apparently for flash plants only. It is evident from the figure that 80% of the reported global capacity emits 200 g or less of GHG per kWh produced. In fact, the weighted average for the global distribution is 122 g/kWh. While the global average is reasonably consistent to the adjusted average of Bloomfield et al (2001), i.e. 106 g/kWh, we are unable to draw any conclusions about the distribution of GHGs from U.S. geothermal facilities. From a GHG emission point of view, it is important to determine the U.S. distribution. After all, though the average value for the global distribution is considerably less than its maximum value, the latter is 50% more than those from a NGCC plant (see Figure 16), a fossil fuel plant.

For estimating the GHG distribution from U.S. geothermal plants, we employed emissions data reported to the California Environmental Protection Agency (CEPA, 2008). However, these data, which are shown in Figure 15, are exclusively from California facilities and as such do not represent the U.S. as a whole. The figure clearly shows that relative to their cumulative capacity, California geothermal GHG emissions distribution ("CA") appears lower than its global distribution counterpart. The California geothermal emissions arise from about 1,800 MW of capacity, which is 90% of U.S. capacity and roughly a quarter of the global capacity (6,800 MW) surveyed by Bertani and Thain. Based on the "CA" distribution shown in Figure 15, we calculated the weighted average for California flash plant data to be 68 g/kWh.
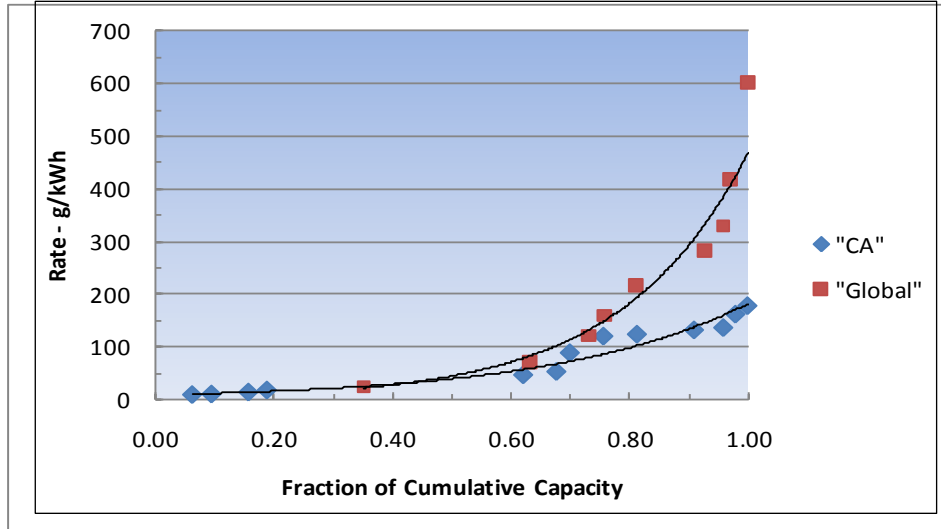
Figure 15   Operational CO$_2$ generation rate from flash plants as a function of the fraction of reported total capacity for global and California production (CEPA, 2008)

Our estimated distribution of GHG emissions from U.S. geothermal facilities must be considered provisional. There are limitations to the California EPA geothermal data arising primarily from inconsistencies in plant emission reporting. Some facilities only report CO$_2$, while others report both CO$_2$ and other GHGs (e.g., methane). And some are not required to report because they are below the absolute emission reporting limit. Finally, the weighted average that we estimated from the "CA" distribution is considerable lower than the adjusted Bloomfield et al (2001) value, which is probably quite reliable. Hence, no firm conclusion can be drawn on differences between the global vs. U.S. emissions distributions shown in Figure 15, other than the global distribution is deemed quite reliable given that 85 facilities in 11 different countries contributed data for that survey.

5.4   LIFE-CYCLE GHGS AMONG THE TECHNOLOGIES

Figure 16 (values in Table A-2) summarizes, by life-cycle stage, our life-cycle GHG emissions estimates (in g/kWh) for the various power technologies considered herein. The figure is consistent with our previous conclusions (Sullivan et al., 2010). Fossil fuel plants generate much more GHGs per kWh than their renewable, hybrid, and nuclear counterparts. As expected, IGCC power is associated with lower GHGs than its conventional counterparts, coal and biomass, respectively. This is a consequence of the greater efficiency of IGCC technologies. For the fossil electricity plants, the preponderance of GHG arises from the fuel burned to produce the electricity.

Figure 16   Greenhouse gas emissions (g/kWh) by life-cycle stage for various power-production technologies relative to total energy output; entries are based on average MPRs given above and GREET 1.8 data.

It is also clear from Figure 16 that all plants have some GHG emissions in their life cycles. For example, GHGs are emitted during nuclear fuel production. More specifically, these GHGs r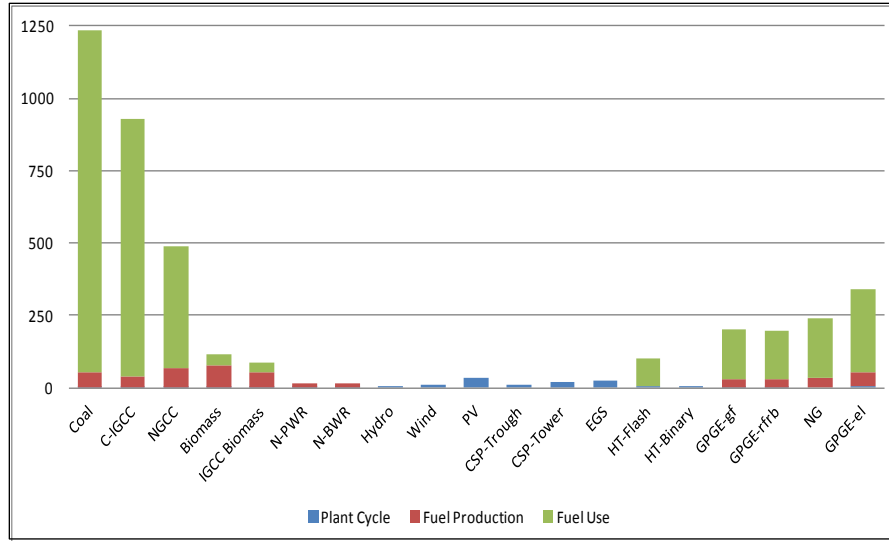esult from fuel use during uranium mining and processing and fuel use and fugitive emissions from natural gas production. The GHGs associated with hydro, wind, PV, CSP, and EGS are all quite small and arise from the plant cycle stage.

Of the renewable and hybrid technologies, hydro, wind, PV, CSP, EGS and HT-Binary are, on balance, the lowest GHG emitters of the technologies covered herein. GPGE, HT-Flash and biomass power have the highest GHG emissions among these technologies, though as seen in Figure 16, they are considerably lower than those from fossil-fuel-based power plants. For HT-Flash, the GHGs are fuel-use emissions and come primarily from dissolved CO_2 in the geofluid that is released to the atmosphere upon its passage through the plant. Though, as discussed in Section 5.3, GHG emissions from an HT-Flash plant could be substantially larger, such a value would represent a particular site and plant and not the U.S. average CO_2 emission level for geothermal power. Also note in the figure that GHGs are emitted during both fuel production and fuel use in biomass-based power, whether from a conventional boiler or an IGCC facility. Most of these GHG emissions are from the fuel production stage, where fuel is used for harvesting forestry residues. Some of the GHGs also arise during fuel use owing to incomplete biomass combustion and associated methane emissions. Nitrous oxide (N_2O) emissions are also generated at that time and contribute to biomass power's GHGs.

As a hybrid technology, GPGE has, as expected, a higher GHG emission rate than those for the renewables, though again small in comparison to those from strictly fossil-based power production. GPGE emissions arise from both natural gas production and use (See Table A-2 for values). For comparison purposes, a bar (NG) has been added to Figure 16, representing the

production of solely natural gas from associated wells. When this bar is compared to those for the GPGE dual-output systems, it is conspicuously higher because its lacks the leveraging effect of the dual output GPGE plants. The electric-power component of the GPGE dual output emissions are very small and arises only from the plant cycle stage. The NG bar is based on GREET 1.8 data for fuel production and use, and plant-cycle CO_2 is based on work by Burnham et al. (2011). For natural gas production, their $\mathcal{E}_{pc}$ and GHG_{pc} values are about an order of magnitude lower than for the lowest electric power plants, thus negligibly contributing to the GHG profile for natural gas output.

Another feature to note in Figure 16 is the insignificant difference in life-cycle GHGs between GPGE-gf and GPGE-rfrb plants, despite their significant difference in GHG_{pc} values. This is because plant-cycle emission is very small in comparison to energy production and use emissions.

In Figure 16, the bar for GPGE-el is clearly higher than that for natural gas production (NG). However, this difference is dependent on a tradeoff between two factors. When compared to just delivering a MW_{th} of produced natural gas, the extra gas needed to produce a MW of electricity is offset in part by the extra electric power derived from the hot geofluid. Indeed, the latter factor is the reason why GHG emissions from GPGE-el are roughly two-thirds of those from the conventional NGCC facility at the left of the figure. Also notice that GPGE-el GHG emissions are about 50% higher than those for GPGE-gf and GPGE-rfrb. This result is due to greater energy output from the dual-output plants vs. the all-electric-output GPGE. Since plant output is defined here as both gas and electric energy delivered to the consumer, gas delivered to a pipeline provides a great energy leverage, thus reducing MPRs and $\mathcal{E}_{pc}$ and GHG_{pc} values, even if the customer uses the gas from the pipeline to generate electricity. (In that case, the burden belongs to the customer and not the plant.)

5.5   THE "OTHER COMBUSTION EMISSIONS"

There are other emissions besides GHGs associated with the production and use of energy products like electricity, coal, natural gas and others. The ones most frequently discussed are NO_x, CO, SO_x, PM, and VOCs. The GREET 1.8 model tracks these emissions for the use and production of a wide range of fuels and electricity generation.

Results from our GREET analysis of criteria pollutant emissions are shown in Figure 17. Because of the range of emission levels, the results are presented on a logarithmic scale. Though GREET 1.8 reports both 2.5- and 10-micron PM, for simplicity the plot shows their sum. From an inspection of the figure, it is clear that the combustion-based electric power-generating technologies, including biomass technologies, shown at the graph's left side, generate 1.5-2 orders of magnitude times those of the other technologies, with the exception of PV and GPGE. In those cases, the difference is somewhat smaller, i.e., about 1−1.5 orders of magnitude. As is evident in Figures 12 and 13 and Table A-2, PV has comparatively high $\mathcal{E}_{pc}$ and GHG_{pc} values when compared to the other renewable technologies.

The emissions for GPGE energy production are shown at the right side of Figure 17. With the exception of biomass electricity production, emissions from dual-output GPGE plants are higher than those from renewable power plants. This result is a direct consequence of GPGE, as a hybrid technology, having a substantial fossil output. On the other hand, as seen in the figure, dual-output GPGE plants have somewhat lower emissions than those facilities that produce only natural gas. The difference between NG and dual-output GPGE is basically related to the latter's ratio of output natural gas energy to the total output energy of the plants. For hybrid facilities, geofluid power output has sensibly no emissions burden and the natural gas output does. As expected, the emissions from natural gas production and direct use are lower than those incurred during NGCC operation (shown at the left). When natural gas is used to produce electricity, the corresponding thermoelectric conversion efficiency requires more gas to be used to generate a kWh of power than used directly to produce an equivalent amount of heat. Finally, for the same reasons given in section 5.4 for GHG emission comparisons, the other combustion emissions for GPGE-el are a little higher than those for direct natural gas use and conspicuously higher (by more than 50%) than those for GPGE-rfrb and GPGE-gf.
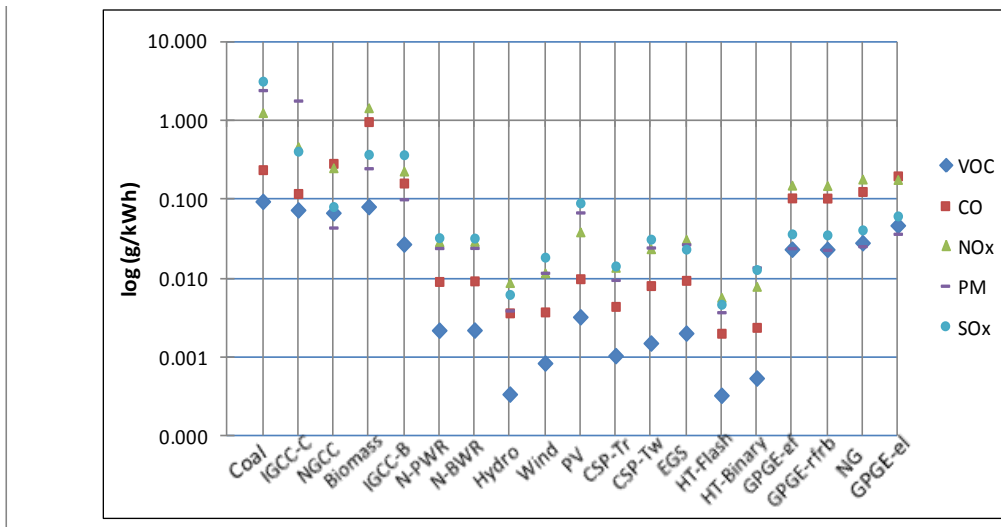
Figure 17   Criteria pollutant emissions (g/kWh) over the life cycles of various power-production technologies.

The significance of the other combustion pollutants is greatly influenced by the locale and region of release. Unlike the GHGs, CO, NO_x, SO_x, PM, and VOC emissions are not considered global emissions and do not persist in the atmosphere for long periods of time. Further, since their primary effect is local, their significance is greatly influenced by whether the region of release is already a "non-attainment" area. In a follow-up report, non-GHG emissions will be discussed in greater detail using updated emissions data currently under development in GREET 1.8.

6 CONCLUSIONS

To expand the scope of our first year's life-cycle assessment of geothermal and other power-generating technologies, we analyzed the life-cycle performance of the following additional systems: GPGE wells that produce both natural gas and electricity, IGCC plants fired by coal and biomass, and CSP plants. We also expanded our analyses of well material and fuel requirements as a function of well depth and technology, established the impact of well-field exploration on well-field life-cycle burdens, estimated the contribution of on-site plant construction activities to E_{pc}, estimated the range of GHG emissions from U.S. geothermal power facilities, and finally, using GREET 1.8 and GREET 2.7, computed non-GHG air-pollutant emissions for various power-production technologies. A detailed discussion of GPGE well construction was also given.

On the basis of our results, a number of conclusions can be drawn:

- Despite their improved efficiency, IGCC power plants have sensibly the same material requirements as other thermoelectric technologies.

- The material requirements for CSP plants are among the highest for all the technologies, whether conventional or renewable.

- Owing to the leveraging effect of dual energy outputs, material requirements for both reworked and green field GPGE plants are lower than for the other geothermal systems. Despite reworked plants having the lowest materials requirements of the two GPGE facilities, both have virtually the same total life cycle GHG emissions.

- Within the design depth for each casing string, the steel and cement requirements for geothermal wells increase linearly with depth.

- The drilling of exploration wells has been estimated to increase overall well material demand by 4–20%, a percentage that decreases with plant capacity.

- On-site plant construction activities contribute about 7% to the plant cycle energy.

- $\mathcal{E}_{pc}$ and GHG_{pc} values are comparable among conventional thermoelectric plants and generally higher for both renewable and hybrid plants.

- A provisional estimation of the GHG emissions distribution from U.S. geothermal plants was made using data of limited quality. However, more reliable data is required for successful determination of this emissions distribution.

- Overall life-cycle GHG emissions for power plants are by far the highest for fossil-based plants and generally considerably lower for renewable and hybrid plants. Owing to their efficiencies, IGCC plants have lower GHG emissions than boiler-based fossil combustion plants. Among the renewable technologies, the highest GHG emitters are HT-Flash and biomass-based electricity.

- GPGE facilities have higher GHG emissions than renewable-technology facilities. This is because they are hybrid plants that produce both natural gas and electricity. Of all the hybrid facilities modeled, the plants that export only electricity from both the geofluid and the natural gas had the highest GHGs and other combustion emissions.

- The "other combustion emissions" are between one and two orders of magnitude greater for combustion-based power generation than for renewable power generation. Generally speaking, these emissions trend the same way as GHG emissions among the power-generating technologies considered.

7 REFERENCES

Bertani, R., and Thain, I., 2001, *Geothermal Power Generating Plant CO$_2$ Emission Survey*, Rev. 1.0, International Geothermal Association, http://www.jeotermaldernegi.org.tr/ian%20i.htm, accessed August 2010.

Blanchard, S. and Reppe, P., 1998, *Life Cycle Analysis of a Residential Home in Michigan*, Center for Sustainable Systems, School of Natural Resources and Environment, University of Michigan, Report No. CSS98-05, September.

Bloomfield, K.K., Moore, J.N., and Neilson, Jr., R.M., 2003, Geothermal Energy Reduces Greenhouse Gases, *Climate Change Research*, March/April, 77–79.

Bourgoyne, A.T., Millheim, K.K., Chenevert, M.E., and Young, Jr., F.S., 1991, *Applied Drilling Engineering*, Society of Petroleum Engineers, Richardson, TX.

Burnham, A., Han, J., Clark, C.E., Wang, M., Dunn, J.B., and Palou-Burnham, I., 2011, Life-Cycle Greenhouse Gas Emissions of Shale Gas, Natural Gas, Coal, and Petroleum, *Environmental Science & Technology*, accepted pending submitted revision.

CEPA, 2008, Air Resources Board, Reported Emissions, Facility Emissions, http://www.arb.ca.gov/cc/reporting/ghg-rep/ghg-rep.htm, accessed August 16, 2011.

Clark, C.E., Harto, C.B., Sullivan, J.L., and Wang, M.Q., 2011a, *Water Use in the Development and Operation of Geothermal Power Plants,* ANL/EVS/R-10/5.

Clark, C.E., Harto, C.B., and Troppe, W.A., 2011b, Argonne National Laboratory, unpublished information.

Cole, R.J., 1999, Energy and Greenhouse Gas Emissions Associated with the Construction of Alternative Structural Systems, *Building and Environment*, 34, 335-348.

Cole, R.J., and Kernan, P.C., 1996, Life Cycle Energy Use in Office Buildings, *Building and Environment*, 31, 307-317.

Fiaschi, D., and Lombardi, D., 2002, Integrated Gasifier Combined Cycle Plant with Integrated CO$_2$-H$_2$S Removal: Performance Analysis, Life Cycle Assessment and Exergetic Life Cycle Assessment, *Int. J. Applied Thermodynamics*, 5(1), 13-24.

GETEM, n.d., Geothermal Electricity Technology Evaluation Model, http://www1.eere.energy.gov/geothermal/getem.html.

IDOT (Illinois Department of Transportation), 2007, Section 1019: Controlled Low-Strength Material (CLSM), *Standard Specifications for Road and Bridge Construction*, 758–760.

Jennejohn, D., 2009, *Research and Development in Geothermal Exploration and Drilling,* Geothermal Energy Association, Washington, D.C.

Knauf Insulation GmBH, 2008, Redi-KladTM 1000° Pipe Insulation, http://www.knaufusa.com/pdf/PE-SS-16_RediKlad1000PipeSS-021208.pdf, accessed August 12, 2011.

Koroneous, C.J., Piperidis, S.A., Tatatzikidis, C.A., and Rovas, D.C., 2008, Life Cycle Assessment of a Solar Thermal Concentrating System, Selected Papers from the WSEAS Conferences in Spain.

Luchini, C., 2011, Personal communication, August.

Mann, M.K., and Spath, P.L., 1997, *Life Cycle Assessment of a Biomass Gasification Combined-Cycle System*, NREL Life Cycle Assessment, http://www.nrel.gov/docs/legosti/fy98/23076.pdf.

Papadopulos, S.S., et al., 1975, Assessment of Onshore Geopressured-Geothermal Resources in the Northern Gulf of Mexico Basin, pp.125-46 in *Assessment of Geothermal Resources of the United States—1975*, Ed. D.E. White and D.L. Williams, U.S. Geological Survey Circular 726.

Peterson, P. F., Zhao, H., and Petroski, R., 2005, *Metal and Concrete Inputs for Several Nuclear Power Plants*, Report UCBTH-05-001.

Randolph, P.L., Hayden, C.G., Mosca, V.L., and Anhaiser, J.L., 1992, *Testing of the Pleasant Bayou Well Through October 1990*, Report by Institute of Gas Technology and Eaton Operating Company for the U.S. Department of Energy, DOE/ID/12578-3-Vol.4, http://www.osti.gov/bridge/servlets/purl/6360574-vIrJCB/native/, accessed March 16, 2011.

Scheuer, C., Keoleian, G.A., and Reppe, P., 2003, Life Cycle Energy and Environmental Performance of a New University Building: Modeling Challenges and Design Implications, *Energy and Buildings*, 35, 1049-1064.

Steinhagen, H.M., and Trieb, F., 2004, *Concentrating Solar Power for Sustainable Electricity Generation, Part 2: Perspectives*, Institute of Technical Thermodynamics, German Aerospace Center (DLR), Stuttgart, Germany, DLR 2004.

Sullivan, J. L., Clark, C. E., Han, J., and Wang, M., 2010, *Life Cycle Analysis Results of Geothermal Systems in Comparison to Other Power Systems*, ANL/ESD 10-5.

Tester, J., et al., 2006, *The Future of Geothermal Energy: Impact of Enhanced Geothermal Systems (EGS) on the United States in the 21st Century*, Massachusetts Institute of Technology, http://geothermal.inel.gov/publications/future_of_geothermal_energy.pdf, accessed August 2010.

USDOE, 1983, *Energy Technology Characterizations Handbook, Environmental Pollution and Control Factors, Third Edition,* DOE/EP–0093, Dist. Category UC–11.

USDOE, 2010, *A History of Geothermal Energy Research and Development in the United States, 1976–2006, Volume 3: Reservoir Engineering*, http://www1.eere.energy.gov/geothermal/pdfs/ geothermal_history_3_engineering.pdf, accessed March 16, 2011.

Viebahn, P., Kronshage, S., Trieb, F., and Lechon, Y., 2008, *D 12.2, Final Report on Technical Data, Costs, and Life Cycle Inventories of Solar Thermal Power Plant*, New Energy Externalities Developments for Sustainability, http://www.needs-project.org/RS1a/RS1a%20D12.2%20Final %20report%20concentrating%20solar%20thermal%20power%20plants.pdf.

Wallace, R.H., et al., 1979, Assessment of Geopressured-Geothermal Resources in the Northern Gulf of Mexico Basin, pp.132-55 in *Assessment of Geothermal Resources of the United States— 1978*, Ed. D.E. White and D.L. Williams, U.S. Geological Survey Circular 790.

APPENDIX A

Table A.1   MPRs for the additional power generating technologies discussed in the present report: material units in tonnes/MW, liters/MW for diesel.

Systems and Refs.	Capacity (MW)	Life-time (yr)	Cap. Fct. (%)	Aluminum	Concrete	Cement	Steel	Diesel	HTF[a]	Thermal Storage	Other	Total Materials
IGCC-Coal												
Fiaschi & Lombardi, 2002[b]	344	15	80		165		34.9				0.51[c]	201
IGCC-Biomass												
Mann and Spath, 1997	115	30	80	0.46	156		58.5				0.68[c]	216
CSP-Trough												
Viebahn et al., 2008	46	30	44		1,303		405	12,229	43[d]	623[e]	133[f]	1,885
Steinhagen et al., 2004	100	25	40		480		250	21,741		300[g]		1,150
CSP-Tower												
Koroneous et al., 2008	1	30	30		1,850		545			none		
Viebahn et al., 2008	15	30	71		2,242		779	7,365		817[h]	212[f]	4,071
GPGE-gf	MW$_{th}$/MW$_e$											
Greenfield Plant	17.3/3.6	30	95	7.8	79.3		38.1	2,836				
Well[i]						64.1	104.1	43,431				
Well-to-Plant[j]					4.2		4.9	2,347				
Totals				7.8	83.5	64.1	1471	48,613				305

Table A-1 (Cont.)

Systems and Refs.	Capacity (MW)	Life-time (yr)	Cap. Fct. (%)	Aluminum	Concrete	Cement	Steel	Diesel	HTF[a]	Thermal Storage	Other	Total Materials
GPGE-rfrb	MW_{th}/MW_e											
Refurbished Field	17.3/3.6	30	95	7.8	79.3		38.1	2,836				
Well[i]						16.8	41.7	5,521				
Well-to-Plant[j]					4.3		6.1	2,347				
Totals				7.8	83.6	16.8	85.9	10,703				192.1

[a]Heat transfer fluid
[b]Though these values represent a plant with CO_2 and H_2S capture, they are likely to be very similar to one without them, as the stripper and absorber are not expected to add appreciably to plant mass, [c]Iron, [d]Thermo-oil, [e]Sodium and potassium nitrate provide 7.5 hr of thermal storage, [f]Glass, [g]Assumed same as e, with 8 hr of thermal storage, [h]Same as e, with 16 hr of thermal storage, [i]Well depth is 5 km, [j]Well-to-plant piping length is 1 km.

Table A.2 **Plant cycle (pc) energy ratios (dimensionless) and components of life cycle GHG emissions (g/kWh) for various power-generating technologies: midrange results in the top rows, maximum and minimum values below.**

	Coal		NGCC	Nuclear		Hydro	Wind	Solar	CSP		Geothermal		
	Pulv	IGCC		PWR	BWR			PV	Trough	Tower	EGS	HTFlash	HTBinary
E_{pc}/E_{out}	0.21%	0.30%	0.11%	0.13%	0.14%	0.85%	2.83%	12.9%	3.39	5.6%	7.62%	1.15%	2.17%
GHG/E_{out}													
pc	0.7	1.12	0.3	0.5	0.6	5.5	9	35.8	10.6	17.9	23.3	4.1	6.1
Fuel prd.	50.4	50.4	67.2	16	16								
Fuel use	1,183	1,183	419.5									98.9	
Total	1,234	1,235	487.0	16.5	16.6	5.5	9	35.8	10.6	17.9	23	103	6.1
Maximum													
E_{pc}/E_{out}	0.28%		0.20%	0.14%	0.15%	1.58%	6.73%	24.2%	3.8%	7.48%	11.60%		
GHG_{pc}/E_{out}	0.92		0.57	0.49	0.68	8.11	21.32	67.7	12.5	23.8	31.9		
Minimum													
E_{pc}/E_{out}	0.11%		0.01%	0.12%	0.12%	0.19%	0.90%	3.26%	3.0%	3.7%	5.5%		
GHG_{pc}/E_{out}	0.32		0.08	0.45	0.60	1.69	2.64	8.35	8.8	12.1	18.6		

TABLE A-2 (Cont.)

	Biomass		GPGE		
	Conv.	IGCC	gf	rfrb	el
E_{pc}/E_{out}	0.22%	0.20%	0.8%	0.4%	1.4%
GHG/E_{out}					
pc	0.7	0.7	2.3	1.1	4.430
Fuel prd.	73.8	73.8	28.7	28.7	46.2
Fuel use	40.6	40.6	168	168	289
Total	115	115	199	198	339
	Maximum				
E_{pc}/E_{out}			0.011	0.005	
GHG_{pc}/E_{out}			3.2	1.3	
	Minimum				
E_{pc}/E_{out}			0.006	0.004	
GHG_{pc}/E_{out}			1.7	1.0	

Energy Systems Division
Argonne National Laboratory
9700 South Cass Avenue, Bldg. 362
Argonne, IL 60439-4815

www.anl.gov